HYDROLOGICAL PROCESSES
Hydrol. Process. **21**, 1616–1623 (2007)
Published online in Wiley InterScience
(www.interscience.wiley.com) DOI: 10.1002/hyp.6724

On the evaluation of snow water equivalent estimates over the terrestrial Arctic drainage basin

Michael A. Rawlins,[1]* Mark Fahnestock,[1,2] Steve Frolking[1,2] and Charles J. Vörösmarty[1,2]

[1] *Water Systems Analysis Group, Institute for the Study of Earth, Oceans, and Space, University of New Hampshire, Durham, NH 03824, USA*
[2] *Department of Earth Sciences, University of New Hampshire, Durham, NH 03824, USA*

Abstract:

Comparisons between snow water equivalent (SWE) and river discharge estimates are important in evaluating the SWE fields and to our understanding of linkages in the freshwater cycle. In this study, we compared SWE drawn from land surface models and remote sensing observations with measured river discharge (Q) across 179 Arctic river basins. Over the period 1988-2000, basin-averaged SWE prior to snowmelt explains a relatively small (yet statistically significant) fraction of interannual variability in spring (April–June) Q, as assessed using the coefficient of determination (R^2). Averaged across all basins, mean R^2s vary from 0·20 to 0·28, with the best agreement noted for SWE drawn from a simulation with the Pan-Arctic Water Balance Model (PWBM) forced with data from the European Centre for Medium-Range Weather-Forecasts (ECMWF) Re-analysis (ERA-40). Variability and magnitude in SWE derived from Special Sensor Microwave Imager (SSM/I) data are considerably lower than the variability and magnitude in SWE drawn from the land surface models, and generally poor agreement is noted between SSM/I SWE and spring Q. We find that the SWE versus Q comparisons are no better when alternate temporal integrations–using an estimate of the timing in basin thaw–are used to define pre-melt SWE and spring Q. Thus, a majority of the variability in spring discharge must arise from factors other than basin snowpack water storage. This study demonstrates how SWE estimated from remote sensing observations, or general circulation models (GCMs), can be evaluated effectively using monthly discharge data or SWE from a hydrological model. Copyright © 2007 John Wiley & Sons, Ltd.

KEY WORDS SWE; river discharge; remote sensing; SSM/I

Received 16 June 2006; Accepted 23 October 2006

INTRODUCTION

Winter snow storage and its subsequent melt are integral components of the climate system. Much remains unknown regarding the magnitudes and interannual variations of this key feature of the Arctic water and energy cycles. Across large parts of the terrestrial Arctic, direct snow observations are unavailable, and this lack of information limits our ability to monitor a region which is exhibiting signs of change (Peterson *et al*., 2002; Vörösmarty *et al*., 2001). Yet, amid declines in Pan-Arctic station observations (Shiklomanov *et al*., 2002), a growing number of models and remote sensing data are being brought to bear for studying the Arctic hydrological cycle. Retrospective analysis or 'reanalysis' of the atmospheric state such as the National Centers for Environmental Prediction (NCEP) and the National Center for Atmospheric Research (NCAR) Reanalysis Project (Kalnay *et al*., 1996) provide benchmark, temporally consistent datasets for water cycle studies. Remote sensing techniques offer the potential for more complete coverage at regional scales (Derksen *et al*., 2003; McDonald *et al*., 2004).

High quality estimates of snow storage and melt can be used to validate the behaviour of hydrological models and general circulation models (GCMs), which have difficulty reproducing solid precipitation dynamics (Waliser *et al*., 2005). Snow cover and snow water equivalent (SWE) estimates are also needed for climate change analysis and flood prediction studies. Approximately 8000 (daily) snow depth observations were analysed to create monthly snow depth and SWE climatologies for North America (Brown *et al*., 2003) for use in evaluating Atmospheric Model Intercomparison Project II (AMIP II) snow cover simulations. Comparisons of continental-scale snow parameters with river discharge time series are useful in improving our understanding of the role of snow accumulation and melt in runoff generation processes. Yang *et al*. (2002), examining the snow-discharge relationship, noted a weak correlation ($R = 0{\cdot}14–0{\cdot}27$) between winter precipitation (a proxy for snow thickness) and streamflow between May and July across the Lena river basin in Siberia. Across the Ob basin, winter snow depth derived from special sensor microwave imager (SSM/I) agrees well with runoff in June ($R = 0{\cdot}61$), with lower correlations for comparisons using May or July discharge (Grippa *et al*., 2005). Strong links have been reported between end-of-winter SWE and spring/early summer river discharge in the Churchill River and Chesterfield Inlet Basins of Northern Canada

* Correspondence to: Michael A. Rawlins, Water Systems Analysis Group, Institute for the Study of Earth, Oceans, and Space, University of New Hampshire, Durham, NH 03824, USA.
E-mail: Rawlins@eos.sr.unh.edu

(Déry *et al*., 2005). Frappart *et al*. (2006) recently compared snow mass derived from SSM/I data and three land surface models with snow solutions derived from Gravity Recovery and Climate Experiment (GRACE) geoid data. GRACE is a geodesy mission to quantify the terrestrial hydrological cycle through measurements of Earth's gravity field. They found that GRACE solutions correlate well with the high-latitude zones of strong accumulation of snow at the seasonal scale.

To better understand the agreement between SWE and observed river discharge, we examine comparisons of their year-to-year changes across 179 river basins over the period 1988–2000. Gridded SWE estimates across the Pan-Arctic drainage basin are taken from both satellite microwave data and land surface model estimates. The objective of our study is to evaluate several common SWE data sets using monthly discharge for watersheds across the terrestrial Arctic basin.

DATA AND METHODS

Spatial, gridded estimates of monthly SWE and discharge for river basins across the Pan-Arctic were analysed for the period 1988–2000. Monthly SWE is drawn from the analysis scheme described by Brown *et al*. (2003) and archived at the Canadian Cryospheric Information Network (CCIN, http://www.ccin.ca); from simulations using the Pan-Arctic Water Balance Model (PWBM) (Rawlins *et al*., 2003); from snowpack water storage in the Land Dynamics Model (LaD) (Milly and Shmakin, 2002); and from SSM/I brightness temperatures (Armstrong and Brodzik, 1995; Armstrong *et al*., 1994). PWBM uses gridded fields of plant rooting depth, soil characteristics (texture, organic content), vegetation, and is driven with daily time series of climate (precipitation (P) and air temperature (T)) variables. Monthly PWBM SWE is obtained from model runs using P and T from 3 different sources (1) ERA-40 (ECMWF, 2002), (2) NCEP-NCAR Reanalysis (NNR) (Kalnay *et al*., 1996), (3) Willmott-Matsuura (WM) (Willmott and Matsuura, 2001). We refer to these SWE estimates as PWBM/ERA-40, PWBM/NNR, and PWBM/WM, respectively. The NNR P data have been adjusted based on a statistical rescaling approach (Serreze *et al*., 2003). Implemented in an effort to minimize biases through the use of observed P data, this method involved (1) interpolation of observed monthly totals from available station records with bias adjustments and (2) disaggregation of the monthly totals to daily totals, making use of daily P forecasts from the NCEP/NCAR Reanalysis. PWBM simulations were performed on the 25×25 km Equal Area Scalable Earth Grid (EASE-Grid) (Brodzik and Knowles, 2002). The LaD has previously been found to explain half of the interannual variance of the runoff/precipitation ratio of 44 major river basins (Shmakin *et al*., 2002). In a study of SWE derived from GRACE and from three LSMs, LaD estimates most closely matched those from GRACE, with a good correspondence at seasonal time scales (Frappart *et al*., 2006). Our analysis also includes SWE (0·25° resolution for years 1988–1997) from the analysis scheme described by Brown *et al*. (2003) and archived at the Canadian Cryospheric Information Network (CCIN, http://www.ccin.ca). LaD SWE at 1° resolution was mapped to the EASE-Grid using inverse-distance weighted interpolation, while CCIN SWE was aggregated to the EASE-Grid using the average of all 0·25° grids falling within each EASE-Grid cell. The PWBM-, LaD-, and SSM/I-derived SWE estimates are Pan-Arctic in nature, i.e. defined at all 39 926 EASE-Grid cells encompassing the Pan-Arctic drainage basin (Figure 1). CCIN SWE are available across EASE-Grid cells over North America only.

Passive microwave radiances from SSM/I–aboard the Defense Meteorological Satellite Program satellite series since 1987–have been used to produce maps of SWE across large regions (Armstrong and Brodzik, 2001; Armstrong and Brodzik, 2002; Derksen *et al*., 2003; Goita *et al*., 2003). Monthly SWE estimated from SSM/I radiances for the period 1988–1999 (on the EASE-Grid) were acquired from the US National Snow and Ice Data Center (M. J. Brodzik, personal communication, 2, March 2004) and are archived under the Arctic RIMS project (http://RIMS.unh.edu). The snow depth algorithm (Armstrong and Brodzik, 2001) is: snow depth (cm) $= 1{\cdot}59 * [(T_{19H} - 6) - (T_{37H} - 1)]$, where T_{19H} is the brightness temperature at 19 GHz and T_{37H} is the brightness temperature at 37 GHz. Water equivalent is obtained from the product of snow depth and density.

Our analysis involves the use of what we term 'pre-melt' SWE (the average of February and March monthly SWE) and spring total Q (the total discharge flow over the months April–June). We chose an average of two months of SWE over one month (or maximal monthly) to better represent mid-winter conditions. The SWE and Q time series are prewhitened to remove any trends prior to the covariance analysis. The Q records are drawn from an updated version of R-ArcticNET (Lammers *et al*., 2001). Although SWE estimates are available for more recent years, our analysis here ends in 2000 due to a lack of more recent river discharge data for river basins across Eurasia. Alternate comparisons using SWE and Q, which vary depending on thaw timing derived from SSM/I data, and by simulated snowmelt, are described in the Results section. In this study, all SWE data sets have valid data at each grid defining the Pan-Arctic drainage basin. For each of the 179 river basins, pre-melt SWE is then determined as an average over all EASE-Grid cells defining the respective basin.

Satellite-borne remote sensing at microwave wavelengths can be used to monitor landscape freeze/thaw state (Ulaby *et al*., 1986; Way *et al*., 1997; Frolking *et al*., 1999; Kimball *et al*., 2001). A step-edge detection scheme applied to SSM/I brightness temperatures (McDonald *et al*., 2004) was used to identify the predominant springtime thaw transition event for each EASE-Grid cell. As with SWE, we derived a basin average date of thaw by averaging thaw event dates across

DOI: 10.1002/hyp

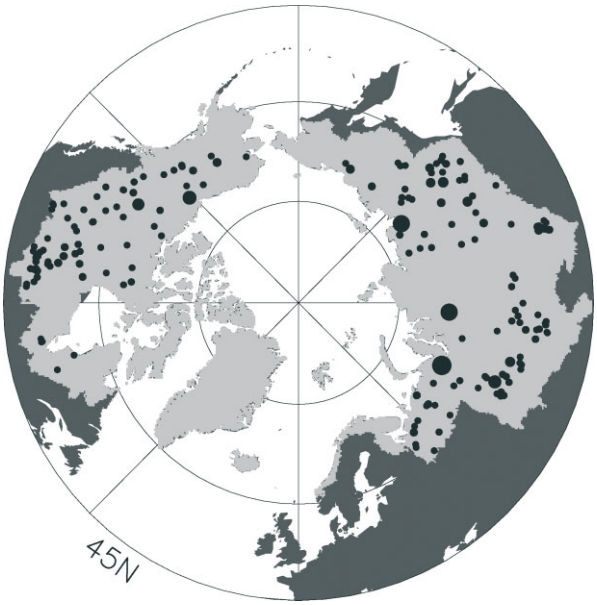

Figure 1. Pan-Arctic land mass (north of 45°N, dark gray), the Arctic drainage basin (light gray), and locations of 179 river basins used in the study. Dot sizes are scaled by basin area. A total of 39 926 EASE-Grid cells comprise the approximately 25 million km^2 drainage basin. Areas for the 179 river basins range from 20 000 km^2 to 486 000 km^2

the basin grid cells. Snow thaw across Arctic basins often can occur over a period of weeks or months. Therefore, for large watersheds, our timing estimates derived from SSM/I brightness temperatures must be interpreted with caution. Nonetheless they provide a general approximation of the timing in landscape thaw for use in estimating pre-melt SWE and spring Q. As an illustration, monthly river discharge, SWE, and thaw date for the Yukon basin are shown in Figure 2a–d.

A simulated topological network (Vörösmarty *et al.*, 2000), recently implemented at 6 min resolution, defines river basins over the approximately 25 million km^2 of the Pan-Arctic basin. The degree to which SWE and Q covary over the period 1988–2000 is evaluated using the coefficient of determination, R^2 (squared correlation). Throughout our analysis, we assume a significance level of 0·05 (5%) as the cutoff to determine whether a given SWE versus Q comparison is statistically significant, and not due to chance. For a sample size of 13 years this corresponds to $R^2 \geq 0{\cdot}22$.

RESULTS

Interannual variability in basin-averaged, pre-melt SWE is compared with spring Q for 179 basins over the period 1988–2000. With the exception of SWE derived from SSM/I data, interannual variability in pre-melt SWE

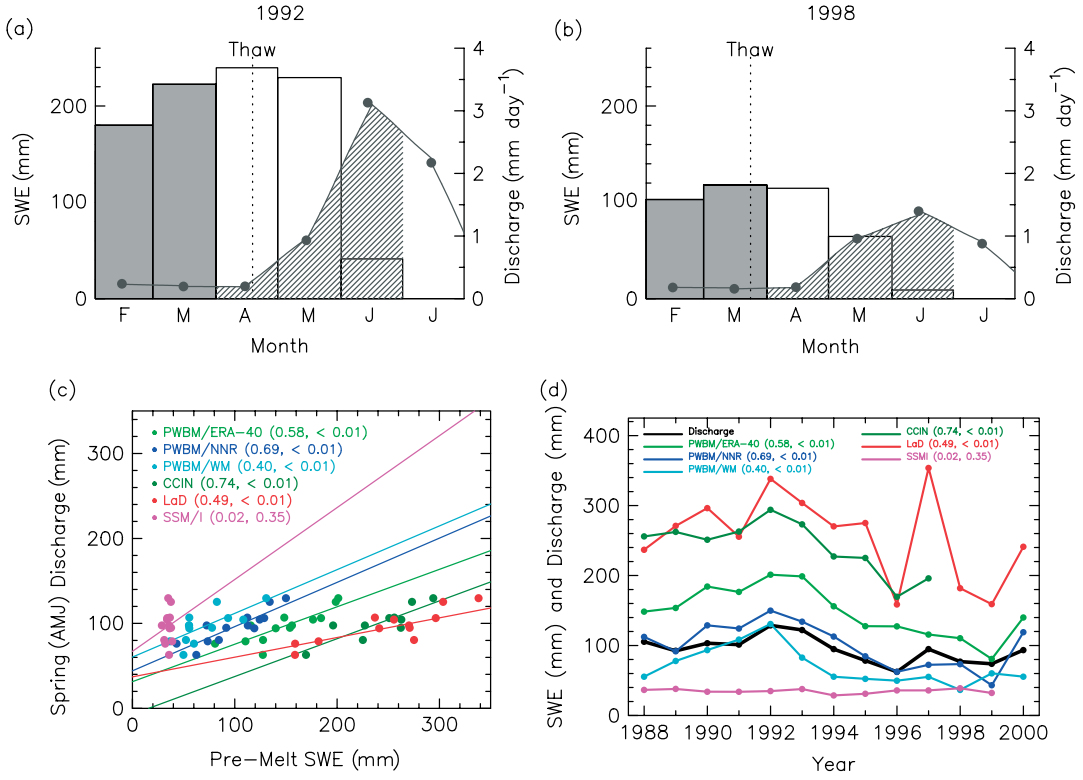

Figure 2. Monthly total SWE (mm) and mean discharge (Q, mm day^{-1}) across the Yukon basin for (a) 1992, a year with relatively high SWE and Q, and (b) 1998, a year with low SWE and Q totals. Vertical bars show SWE–in this case from PWBM driven with ERA-40 data (PWBM/ERA-40). February and March SWE values (gray bars here) are averaged to give 'pre-melt' SWE in this study. April–June SWE are depicted by white bars. Spring Q (monthly values indicated by dots at middle of month) is the integration of the monthly Q for April through June (hatched area), and is used for comparisons with the pre-melt SWE. A 'thaw date' (marked Thaw) estimated from SSM/I data are used in alternate Q integrations. SWE is aggregated across all grid cells upstream of the gauge at Eagle, AK. Basin area for Yukon River at Eagle, AK is 293 965 km^2. R-ArcticNet river discharge volumes are converted to a unit depth (volume/basin area). (c) Scatterplot of pre-melt SWE from each data set, for years 1988-2000. The CCIN and SSM/I estimates are available up to years 1997 and 1999 respectively. The best fit line based on linear least squares regression is shown. (d) Time series of SWE and Q. Statistics (R^2 and associated p-value) for each covariance comparison are shown in parenthesis

DOI: 10.1002/hyp

agrees well with spring Q variability across the Yukon basin in Alaska (Figure 2). Variability in basin SWE from the CCIN analysis scheme explains nearly 75% of the variability in spring Q. When the PWBM is forced with reanalysis data (PWBM/ERA-40 or PWBM/NNR), pre-melt SWE explains well over 50% of the variability in spring Q. Across the Yukon basin, the greater SWE variability and magnitude (among all SWE products) is noted for LaD SWE, along with a lower R^2 (Figure 2c–d). Basin averaged SWE derived from SSM/I, however, shows little interannual variability and relatively low magnitude. For snow packs above 100 mm, the bias in SWE estimated from Scanning Multichannel Microwave Radiometer (SMMR) data was shown to be linearly related to the snow pack mass, with root-mean-square errors approaching 150 mm (Dong *et al*., 2005).

In contrast to the result over the Yukon basin, strong agreements in pre-melt SWE and spring Q variability are not noted across many of the study basins. Although R^2s for a majority of the North American basins are significant (mean values between 0·26 and 0·36, Table I), agreements across western Eurasia are generally low (Figure 3, Table I). Of the comparisons involving SWE from PWBM, more than half (130 of 231) are significant. Mean R^2s from comparisons using the PWBM are comparable to those involving CCIN SWE estimates, which were developed using observed snow depth observations (Brown *et al*., 2003). Across all basins analysed, the highest proportion of negative correlations (very poor agreement) and lowest overall R^2 are associated with SSM/I SWE. The algorithm used to produce these estimates, like many of the early passive-microwave SWE algorithms, tends to underestimate SWE in forested regions. Models which account for the differing influences on the microwave signature have shown promise in reducing errors in forested regions (Goita *et al*., 2003). The best agreements involving SSM/I SWE are found across the prairies of south-central Canada. This is expected, as the SSM/I SWE algorithm was developed for application across the non-forested prairie provinces of Canada.

Comparisons using SWE from the PWBM simulations (PWBM/ERA-40, PWBM/NNR, and PWBM/WM), produce similar R^2 values across each region, with mean value by region ranging from 0·15 to 0·36. Given that water budget models like PWBM are most sensitive to time-varying climatic inputs (Rawlins *et al*., 2003), small differences in R^2 among these SWE estimates suggest similar spatial and temporal variability among the underlying precipitation data. Basin R^2s obtained from comparisons using LaD SWE are comparable with those from the comparisons using PWBM SWE across North America, while lower correlations are noted for Eurasia. Mean R^2s are higher across eastern Eurasia (east of longitude 90 °E) as compared with western Eurasia. The better agreement across Siberia is likely attributable to the higher fraction of precipitation which falls as snow and the higher discharge/precipitation ratios across the colder east. When the PWBM is driven with precipitation data from a new gauge-corrected archive for the former USSR ('Daily and Sub-daily Precipitation for the Former USSR') National Climatic Data Center, 2005, basin R^2s are generally no higher (figure not shown). This suggests that precipitation-gauge under catch is not a significant influence on the computed SWE versus Q agreements.

Snowmelt and subsequent rises in river Q begins in southerly regions of the terrestrial Arctic and progresses northward each spring. Comparisons of winter SWE storage and Q over a fixed interval (e.g. April–June) are

Table I. Mean February–March SWE (mm), negative correlations, and minimum, maximum, and mean coefficient of determination (R^2) from the pre-melt SWE and spring Q comparisons. SWE is taken from data sets described in Data and Methods and shown in Figure 3. Percentage of negative correlations, and mean coefficient of determination is also tabulated for simulated spring Q versus observed spring Q (row SimRO), where simulated Q is from PWBM/ERA-40 model simulation. Mean February-March SWE is averaged across the terrestrial Arctic basin, excluding Greenland. Individual R^2 values for each study basin (shown in Figure 3) are averaged (excluding negative correlations) over all 179 river basins (All), and the basins across North America, western Eurasia, and eastern Eurasia, with the latter two separated by the 90 °E meridian. Mean R^2 for CCIN SWE are determined for North American sector only. PWBM/ERA-40[a–e] represent the alternate comparisons, defined in Section 3

SWE Data	Feb–Mar SWE (mm)	Min, Max, and Mean Coefficient of Determination, R^2				
		% neg.	All	North Am.	W. Eurasia	E. Eurasia
CCIN	N/A	15·6	N/A	0·00, 0·87, 0·35	N/A	N/A
PWBM/ERA-40	103	8·5	0·00, 0·91, 0·28	0·00, 0·91, 0·36	0·00, 0·45, 0·15	0·00, 0·66, 0·27
PWBM/NNR	109	12·6	0·00, 0·87, 0·25	0·00, 0·87, 0·33	0·00, 0·56, 0·15	0·00, 0·71, 0·23
PWBM/WM	109	11·9	0·00, 0·91, 0·26	0·00, 0·91, 0·33	0·00, 0·75, 0·22	0·00, 0·53, 0·17
LaD	144	20·1	0·00, 0·83, 0·24	0·00, 0·83, 0·33	0·00, 0·49, 0·12	0·00, 0·69, 0·16
SSM/I	80	72·1	0·00, 0·76, 0·20	0·00, 0·76, 0·26	0·00, 0·40, 0·10	0·00, 0·57, 0·14
SimRO	103	5·3	0·00, 0·92, 0·46	0·01, 0·91, 0·44	0·00, 0·79, 0·35	0·05, 0·92, 0·57
PWBM/ERA-40[a]	103	10·0	0·00, 0·80, 0·27	0·00, 0·80, 0·33	0·00, 0·61, 0·22	0·00, 0·64, 0·22
PWBM/ERA-40[b]	103	18·7	0·00, 0·93, 0·34	0·00, 0·93, 0·37	0·00, 0·86, 0·38	0·00, 0·70, 0·26
PWBM/ERA-40[c]	103	10·0	0·00, 0·80, 0·27	0·80, 0·00, 0·33	0·61, 0·00, 0·22	0·00, 0·64, 0·22
PWBM/ERA-40[d]	103	10·0	0·00, 0·80, 0·27	0·80, 0·00, 0·33	0·61, 0·00, 0·22	0·00, 0·64, 0·22
PWBM/ERA-40[e]	103	22·8	0·00, 0·76, 0·25	0·00, 0·76, 0·35	0·00, 0·28, 0·12	0·00, 0·58, 0·19

DOI: 10.1002/hyp

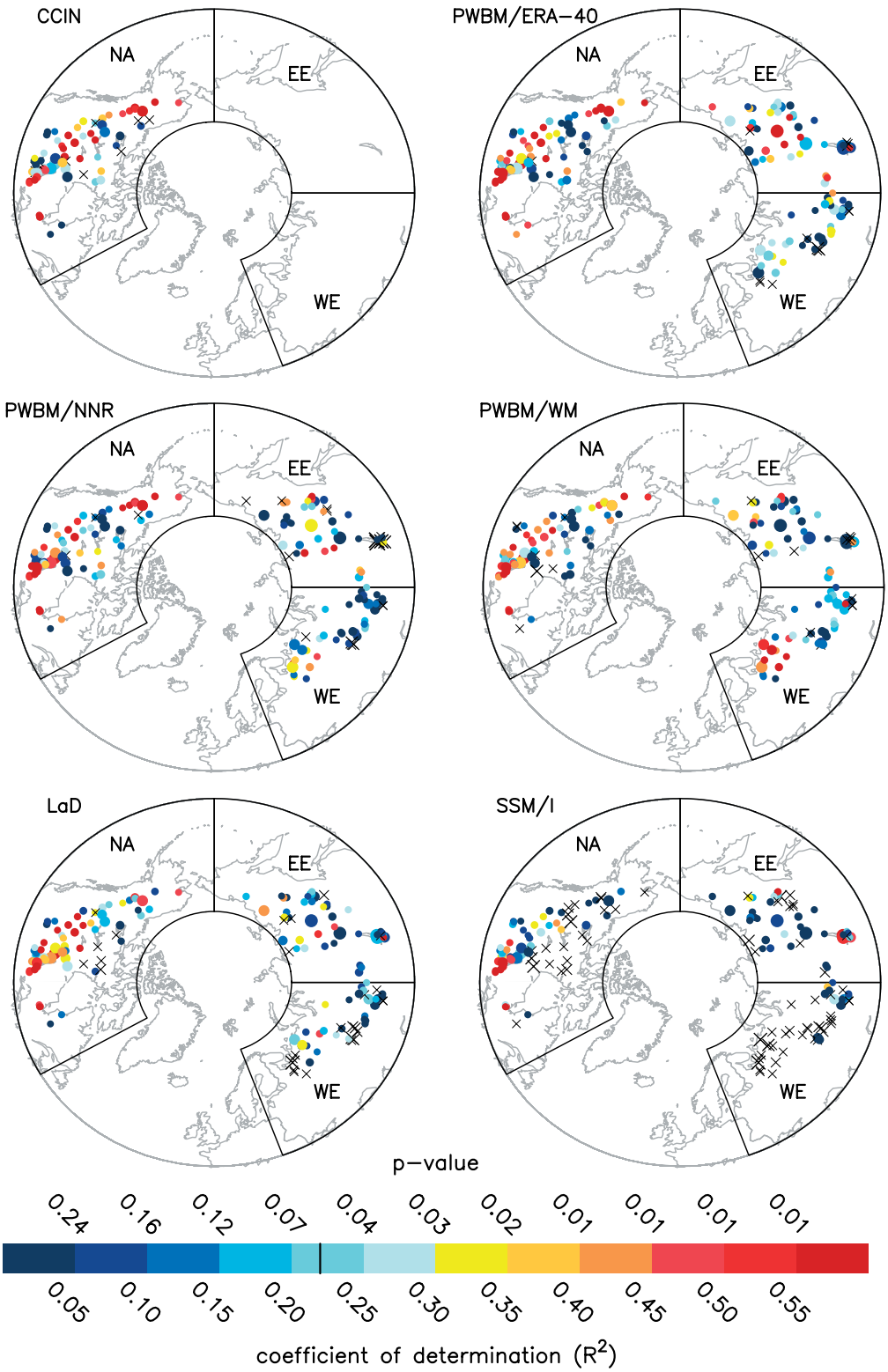

Figure 3. Coefficient of determination (R^2) for pre-melt SWE and spring Q comparisons (1988–2000) at the 179 river basins and for the 6 SWE products. SWE is taken from the CCIN SWE analysis; PWBM simulations driven by ERA-40, NNR and WM; LaD model; and SSM/I data. The 'X's mark basins with a negative correlation. Average R^2 values across all basins, North America (NA), western Eurasia (WE), and eastern Eurasia (EE) are shown in Table I. The vertical line in colorbar is level ($R^2 = 0{\cdot}22$) at which R^2 is significant at 5% level. P-values associated with each R^2 interval are shown above the colorbar. Note that $p < 0{\cdot}01$ for all $R^2 \geq 0{\cdot}40$

complicated when inputs from rainfall are significant, or a large fraction of the snowmelt occurs outside of the April–June period. A more meaningful comparison of SWE and river Q would be restricted to that fraction of Q which is attributable to the melting of snow. For example, simulated spring Q from PWBM—driven by ERA-40 data–explains a much higher proportion of observed spring Q than does the pre-melt SWE across the study

DOI: 10.1002/hyp

basins (Figure 4, Table I). The correspondence between simulated and observed spring Q suggests the model—to some degree–is accounting for processes connecting the snowpack and spring river flow, e.g. sublimation, rainfall, and soil infiltration.

To better understand the covariance between SWE and Q, alternate comparisons were made using PWBM/ERA-40 monthly SWE and an estimate of when thaw is assumed to have occurred. The month of thaw (TM, with $TM-1$, and $TM+1$ indicating the month preceding and succeeding the thaw month, respectively) was determined with a step edge detection scheme applied to SSM/I brightness temperatures (McDonald *et al*., 2004). Then, SWE_{TM} becomes monthly basin SWE during TM (or $TM-1$), and Q_{TM} is discharge in month TM. These alternate comparisons (across all 179 basins) are defined (1) SWE_{TM} versus spring Q, (2) $SWE_{\mathrm{TM-1}}$ versus spring Q, (3) $SWE_{\mathrm{TM-1}}$ versus $Q_{\mathrm{TM+1}}$, (4) $SWE_{\mathrm{TM-1}}$ versus $Q_{\mathrm{TM+1,2}}$. R^2s are highest for alternate comparison (2), which compared SWE in the month before thaw ($TM-1$) with spring (April–June) Q (Table I). Yet, despite the fact that the mean R^2 across western Eurasia improves from 0·15 (pre-melt SWE versus spring Q) to 0·38 (alternate comparison b), little difference is noted with the remianing alternate comparisons and other regions.

Lastly, we scaled spring Q using a factor S, where S = PWBM monthly snow melt–runoff ratio, with $0 < S < 1$. Then, snowmelt Q each month is $Q_s = Q{\cdot}S$. Each occurrence of Q_S was then summed resulting in a total Q_S each spring, for each basin. Using Q_S in place of the default Q (and PWBM/ERA-40 SWE), we note a decrease in agreement across eastern Eurasia, with no change across most of the domain. And although SWE from simulations with ERA-40, in general, explains more than a third of the variation in Q, a large proportion of the interannual variability is not due to SWE variability. When considering these results, it is interesting to note that Lammers *et al*. (2006) recently found that annual simulated discharge across Alaska (drawn from three separate models) was in poor agreement with observed discharge data between 1980–2001. Better agreements across northwestern North America, eastern Eurasia (EE in Figure 3), and parts of western Eurasia (WE) in this study are attributable to relatively higher snowfall rates and a greater interannual variability in spring discharge (Figure 4b). Conversely, the region of western Eurasia with numerous negative correlations is characterized by low spring discharge variability. Delays in snowmelt water reaching river systems, which can be significant (Hinzman and Kane, 1991), are likely an additional influence on these reported correlations. For large Arctic basins, comparisons between snow storage and discharge volume are complicated by the large temporal variation in basin thaw and the delays in snowmelt water reaching the gauge. More meaningful comparisons between spatial SWE and river discharge are possible through the use of hydrograph separation to partition discharge into overland and baseflow components. This, however, requires the use of daily discharge data which are more limited for the Pan-Arctic region.

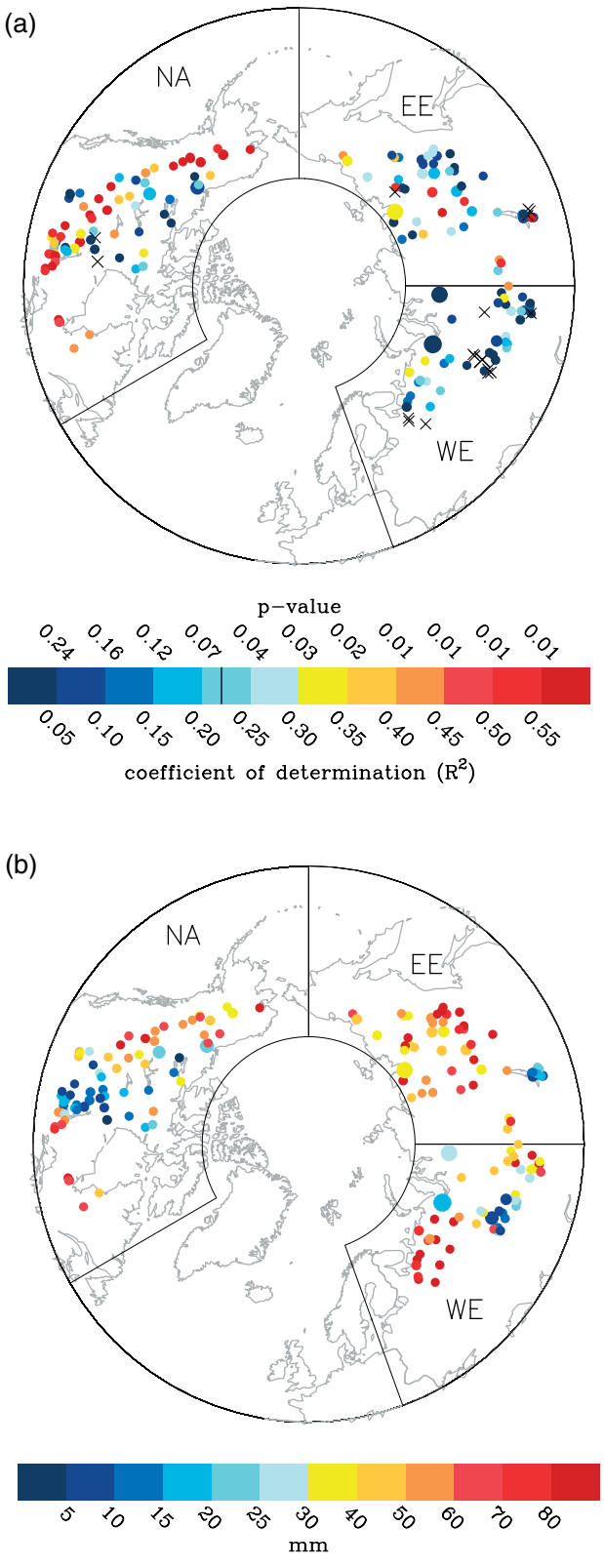

Figure 4. (a) R^2 for PWBM simulated spring total Q versus observed spring total Q. The vertical line in colorbar is level at which R^2 is significant. Minimum, maximum, and mean R^2s across all basins, North America (NA), western Eurasia (WE), and eastern Eurasia (EE) are shown in Table I. The 'X's mark basins with a negative correlation. (b) Standard deviation of spring (April–June) discharge for the period 1988–2000

DOI: 10.1002/hyp

CONCLUSIONS

In our comparisons of interannual variations in pre-melt SWE and spring Q, R^2 values are highest (mean of 0·25 to 0·28 over all basins) when PWBM is driven by ERA-40, NNR or WM climate data. Similar agreements are noted when SWE from the observed data analysis scheme are used, which suggests that the hydrological model is capturing as much variability in the spring flow as does the observed SWE scheme. Average R^2 determined from the SSM/I SWE and spring Q comparisons are generally low, and a sizable majority (over 72%) of these correlations are negative. The low variability and magnitude is likely related to saturation of the SSM/I algorithm at high SWE values. Continued development of new regional algorithms which account for microwave emmission from forests should improve large-scale SWE estimates. Poor agreements among all SWE products–particularly across parts of western Eurasia–are noted in areas with low discharge variability. Pre-screening to eliminate basins with low flow or insufficient variability would likely improve the SWE versus Q agreements.

Results of the covariance analysis using alternate temporal integrations to derive pre-melt SWE (or Q) suggest that our choice of a fixed interval for spring, i.e. April–June, is not the primary cause of the relatively low R^2s. Furthermore, we conclude that much of the interannual variability in river discharge must be influenced by factors other than basin SWE storage variations. The unexplained variability is likely due to a combination of effects from physical processes (sublimation, infiltration) and errors in spatial SWE. Relatively good agreement between simulated and observed spring Q suggests that hydrological models can be useful in understanding the SWE-to-Q linkages. Our results provide a benchmark of the relationship between the solid precipitation input and spring discharge flux, and demonstrate that hydrological models driven with reanalysis data can provide SWE estimates sufficient for use in validation of remote-sensing and GCM SWE fields. Additional studies using daily discharge data to better quantify snowmelt runoff will further facilitate SWE product evaluations and the understanding of linkages in the Arctic hydrological system.

ACKNOWLEDGEMENTS

The authors thank Richard Lammers, Ernst Linder, and Dominik Wisser (University of New Hampshire) and Cort Willmott (University of Delaware) for frequent useful discussions, and Kyle McDonald (Jet Propulsion Laboratory) for the thaw timing data. We also thank Chris Milly for providing the LaD SWE estimates. This study was supported by the NSF ARCSS program and NSF grants OPP-9910264, OPP-0230243, OPP-0094532, and NASA grant NAG5-9617. SWE and river discharge data used in this study are available upon request from the Water Systems Analysis Group (watsys@unh.edu).

REFERENCES

Armstrong RL, Brodzik MJ. 1995. An earth-gridded SSM/I data set for cryospheric studies and global change monitoring. *Advances in Space Research* **16**(10): 155–163.

Armstrong RL, Brodzik MJ. 2001. Recent Northern Hemisphere snow extent: a comparison of data derived from visible and microwave sensors. *Geophysical Research Letters* **28**(19): 3673–3676.

Armstrong RL, Brodzik MJ. 2002. Hemispheric-scale comparison and evaluation of passive-microwave snow algorithms. *Annals of Glaciology* **34**(1): 38–44.

Armstrong RL, Knowles KW, Brodzik MJ, Hardman MA. 1994, updated current year. DMSP SSM/I Pathfinder daily EASE-Grid brightness temperatures, 1988–1999. National Snow and Ice Data Center: Boulder, Colorado, USA (digital media).

Brodzik MJ. 2004. personal communication, 2 March, 2004.

Brodzik MJ, Knowles K. 2002. EASE-Grid: a versatile set of equal-area projections and grids. In *Discrete Global Grids*, Goodchild M (ed.). National Center for Geographic Information and Analysis: Santa Barbara, CA.

Brown RD, Brasnett B, Robinson D. 2003. Gridded North American monthly snow depth and snow water equivalent for GCM evaluation. *Atmosphere-Ocean* **41**(1): 1–14.

Derksen C, Walker A, LeDrew E, Goodison B. 2003. Combining SMMR and SSM/I data for time series analysis of central North American snow water equivalent. *Journal of Hydrometeorology* **4**(2): 304–316.

Déry SJ, Sheffield J, Wood EF. 2005. Connectivity between Eurasian snow cover extent and Canadian snow water equivalent and river discharge. *Journal of Geophysical Research* **110**(D23): D23106, Doi:10·1029/2005JD006173.

Dong J, Walker JP, Houser PR. 2005. Factors affecting remotely sensed snow water equivalent uncertainty. *Remote Sensing of Environment* **97**: 68–82.

European Centre for Medium Range Weather Forecasts (ECMWF). 2002. ERA-40 Project Report Series. 3. Workshop on Re-analysis, 5–9 november 2001. Technical report, European Centre for Medium Range Weather Forecasts, 443.

Frappart F, Ramillien G, Biancamaria S, Mognard NM, Cazenave A. 2006. Evolution of high-latitude snow mass derived from the GRACE gravimetry mission (2002–2004). *Geophysical Research Letters* **33**: L02501, Doi:10·10292005GL024778.

Frolking S, McDonald KC, Kimball J, Way JB, Zimmermann R, Running SW. 1999. Using the space-borne NASA scatterometer (NSCAT) to determine the frozen and thawed seasons of a boreal landscape. *Journal of Geophysical Research* **104**(D22): 27,895–27,907.

Goita K, Walker AE, Goodison BE. 2003. Algorithm development for the estimation of snow water equivalent in the boreal forest using passive microwave data. *International Journal of Remote Sensing* **24**(5): 1097–1102.

Grippa M, Mognard N, Toana TL. 2005. Comparison between the interannual variability of snow parameters derived from SSM/I and the Ob river discharge. *Remote Sensing of Environment* **98**: 35–44.

Hinzman LD, Kane DL. 1991. Snow hydrology of a headwater Arctic basin 2. Conceptual analysis and computer modeling. *Water Resources Research* **27**(6): 1111–1121.

Kalnay E, Kanamitsu M, Kistler R, Collins W, Deaven D, Gandin L, Iredell M, Saha S, White G, Woolen J, Zhu Y, Chelliah M, Ebisuzaki W, Higgens W, Janowiak J, Ropelewski KC, Wang J, Leetma A, Reynolds R, Jenne R, Joseph D. 1996. The NCEP/NCAR 40-year reanalysis project. *Bulletin of the American Meteorological Society* **77**: 437–471.

Kimball JS, McDonald KC, Keyser AR, Frolking S, Running SW. 2001. Application of the NASA scatterometer (NSCAT) for determining the daily frozen and nonfrozen landscape of Alaska. *Remote Sensing of Environment* **75**: 113–126.

Lammers RB, Shiklomanov AI, Vörösmarty CJ, Fekete BM, Peterson BJ. 2001. Assessment of contemporary Arctic river runoff based on observational discharge records. *Journal of Geophysical Research* **106**(D4): 3321–3334.

Lammers RB, Rawlins M, McGuire D, Clein J, Kimball J, Wu W. 2006. Water budget closure over the western arctic and Yukon river basin—a model inter-comparison. *Earth Interactions* (in press).

McDonald KC, Kimball JS, Njoku E, Zimmermann R, Zhao M. 2004. Variability in springtime thaw in the terrestrial high latitudes: monitoring a major control on biospheric assimilation of atmospheric CO_2 with spaceborne microwave remote sensing. *Earth Interactions* **7**: 1–23.

Milly PCD, Shmakin AB. 2002. Global modeling of land water and energy balances: I. The Land Dynamics (LaD) model. *Journal of Hydrometeorology* **3**: 283–299.

National Climatic Data Center. 2005. Daily and Sub-daily Precipitation for the Former USSR, Technical report-9813. Available from National Geophysical Data Center: http://www.ncdc.noaa.gov/oa/document-library/ surface-doc.html9813.

Peterson BJ, Holmes RM, McClelland JW, Vörösmarty CJ, Lammers RB, Shiklomanov AI, Shiklomanov IA, Rahmstorf S. 2002. Increasing river discharge to the Arctic Ocean. *Science* **298**: 2171–2173.

Rawlins MA, Lammers RB, Frolking S, Fekete BM, Vörösmarty CJ. 2003. Simulating pan-Arctic runoff with a macro-scale terrestrial water balance model. *Hydrological Processes* **17**: 2521–2539.

Serreze MC, Clark MP, Bromwich DH, Etringer AJ, Zhang T, Lammers R. 2003. Monitoring precipitation over the Arctic terrestrial drainage system: Data requirements, shortcomings, and applications of atmospheric reanalysis. *Journal of Hydrometeorology* **4**(2): 387–407.

Shiklomanov AI, Lammers RB, Vörösmarty CJ. 2002. Widespread decline in hydrological monitoring threatens Pan-Arctic research. *EOS Transactions-American Geophysical Union* **83**(2): 13–17.

Shmakin AB, Milly PCD, Dunne K. 2002. Global modeling of land water and energy balances. part III: Interannual variability. *Journal of Hydrometeorology* **3**(3): 311–321.

Ulaby FT, Moore RK, Fung AK. 1986. *Microwave Remote Sensing: Active and Passive, Vol. III—Volume Scattering and Emission Theory, Advanced Systems and Applications*. Artec House Inc.: Dedham, MA.

Vörösmarty CJ, Fekete BM, Maybeck M, Lammers RB. 2000. Geomorphometric attributes of the gloabl system of rivers at 30-min spatial resolution. *Journal of Hydrology* **237**: 17–39.

Vörösmarty CJ, Hinzman LD, Peterson BJ, Bromwich DH, Hamilton LC, Morrison J, Romanovsky VE, Sturm M, Webb RS. 2001. The hydrologic cycle and its role in arctic and global environmental change: A rationale and strategy for synthesis study. Technical report, Fairbanks, AK: Arctic Research Consortium of the U.S.

Waliser DE, Waliser SE, Seo K, Enjoku E. 2005. Evaluation and climate change projections of the global hydrological cycle in IPCC AR4 model simulations. *Eos Transactions-American Geophysical Union* **86**: Fall Meet. Suppl., Abstract H51I-07.

Way JB, Zimmermann R, Rignot E, McDonald K, Oren R. 1997. Winter and spring thaw as observed with imaging radar at BOREAS. *Journal of Geophysical Research* **102**(D24): 29673–29684.

Willmott CJ, Matsuura K. 2001. Arctic terrestrial air temperature and precipitation: monthly and annual time series (1930–2000) version 1. Available online at: http://climate.geog.udel.edu/~climate/.

Yang D, Kane DL, Hinzman LD. 2002. Siberian Lena River hydrologic regime and recent change. *Journal of Geophysical Research* **107**(D23): 4694, Doi:10·1029/2002JD002542.